

# TESTING OF A MODERN TRANSPORT AIRCRAFT CONFIGURATION IN ETW CLOSE TO MACH 0.9

**Jürgen Quest, Martin C.N. Wright**  
**European Transonic Windtunnel GmbH**  
**Ernst-Mach-Straße, D-51147 Köln, Germany**

**Stephen Rolston**  
**Airbus UK, Filton House, Bristol, UK**

**Keywords:** *High Reynolds number, Transonic wind tunnel testing*

## Abstract

*The European Transonic Windtunnel (ETW) provides the capability for achieving full scale flight Reynolds numbers by testing up to high pressures (450 kPa) and cryogenic (down to 110 K) temperatures. Within the scope of the 'HiReTT' European research programme a modern transport aircraft configuration has been tested over a large range of aerodynamic conditions. 'HiReTT' is specifically devoted to gain high quality data in the high Mach number and high Reynolds number range. The programme has therefore included a sting supported test series together with a complementary series of tests using twin sting supports to accurately assess sting effects. ETW's standard twin sting rig (TSR) has been improved by developing an enhanced version (ETSR) incorporating twin six component balances.*

*This paper describes the development and calibration of the new support system, the design and manufacture of model related components, and provides an overview of the complete programme of wind tunnel tests.*

## 1 Introduction

The collaborative research project HiReTT (**H**igh **R**eynolds Number **T**ools and **T**echniques for Civil Aircraft Design) is focused on understanding the effects of scale on aircraft drag. The project was launched in January 2000 as part of the European Fifth Framework Programme. The purpose of the HiReTT programme is to deliver to the European aerospace industry a capability to accurately predict aircraft flight performance before product launch and to be able to exploit the benefits of designing at flight Reynolds number. The work described in this paper covers the initial phases of the experimental investigations and encompasses the following principal objectives from the complete HiReTT programme:

- To obtain high quality experimental data for a modern aircraft research configuration with and without control devices, at flight representative Reynolds numbers;
- To derive accurate sting interference effects using the standard and enhanced twin sting techniques and to assess the merits of these methods for closely coupled wing-fuselage configurations in ETW;

The programme of work described in this paper forms only a part of the entire project and more complete details are provided separately [1,2].

## 2 Single Sting Tests

The first experimental investigations to be performed within the HiReTT project were the single sting tests. These tests used an existing wind tunnel model, supplied by Airbus UK, with free and fixed transition across a Reynolds number range of 4-42 million. The test programme was devised so as to separate the Reynolds number and wing deformation effects and measurements included forces, moments, surface pressures, transition detection as well as wind tunnel wall pressures.

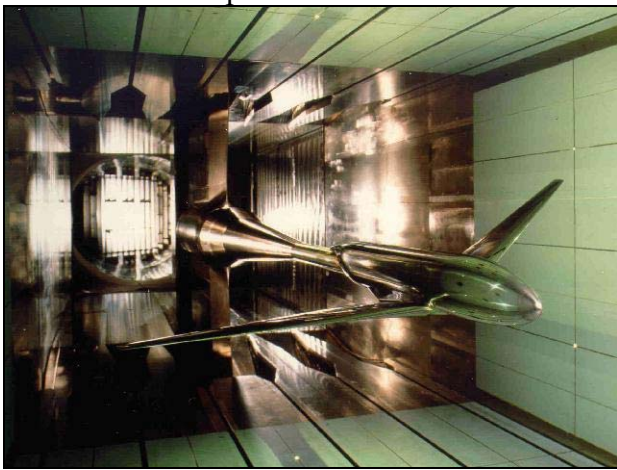


Figure 1 Model in the test section at ETW

A general view of the model installed in the test section at ETW is shown in Figure 1. The model was equipped with pressure plotting at seven spanwise stations and these pressures were measured simultaneously with the forces and moments. These were measured with a high quality six component balance which had previously been calibrated over the complete range of temperature and load conditions. To enable testing over the wide range of conditions possible at ETW the majority of the model components had been manufactured from Maraging steel. Special attention [3] had been taken during the design phase to ensure that the model quality was maintained, even under the most severe case of low temperature and high pressure.

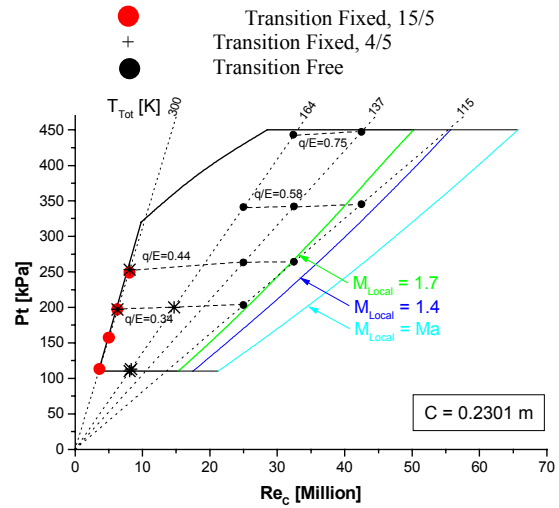


Figure 2 Single sting test conditions at Mach 0.85

The range of test conditions covered during this phase is shown in Figure 2. From this figure it can be seen that the tests included transition fixed conditions at low Reynolds numbers together with transition free conditions at Reynolds numbers above 25 million. The tests included a range of Mach numbers and variations of Reynolds numbers with constant wing shape (constant  $q/E$ ), and variations of  $q/E$  at constant Reynolds number.

### 2.1 Infrared Transition Detection

In addition to obtaining forces, moments, and pressures data a series of Infrared images were recorded at Reynolds numbers in the range 5-25 million. To prepare the model for this part of the test programme a coating was applied to both the upper and lower sides of the wing surfaces with the exception of the leading edges (first 3%) and the pressure plotting rows. A photograph of the leading edge region is provided in Figure 3. The coating adopted for this technique was selected based on previous experience at ETW [4]. In the region of the leading edges and each of the pressure plotting stations the target was to achieve a smooth blend between the coating and the metallic surfaces and aim to keep the overall surface roughness to less than  $Ra=0.2\mu\text{m}$ .



Figure 3 Model preparation for infrared testing

ETW operates two infrared systems, both capable of installation in the test section top wall structure. The first system is a standard AGEMA Thermovision 1000 camera which can be operated at temperatures down to 210 K. The second system, known as CRYSTAL (CRYogenic System for Thermographic Analysis of aerodynamic Layers), can be operated at temperatures down to 100 K. Each camera system was used during this test series and an example of a processed image is provided in Figure 4.



Figure 4 Typical infrared image

The IR images confirmed the development of the boundary layer over a wide range of test conditions. At the highest Reynolds numbers the images proved that transition was either at or very close to the wing leading edge. At the

intermediate Reynolds number shown in Figure 4 the CRYSTAL camera system confirmed that pockets of laminar flow were still clearly visible. This was an encouraging result both in terms of the test technique and also in terms of demonstrating the flow quality at ETW.

### 2.3 Short Term Repeatability

A small number of repeat conditions were built into the test programme to confirm data quality. A typical example of the short-term repeatability is provided in Figure 5, which includes 2 continuous traverse polars together with a pitch and pause polar.

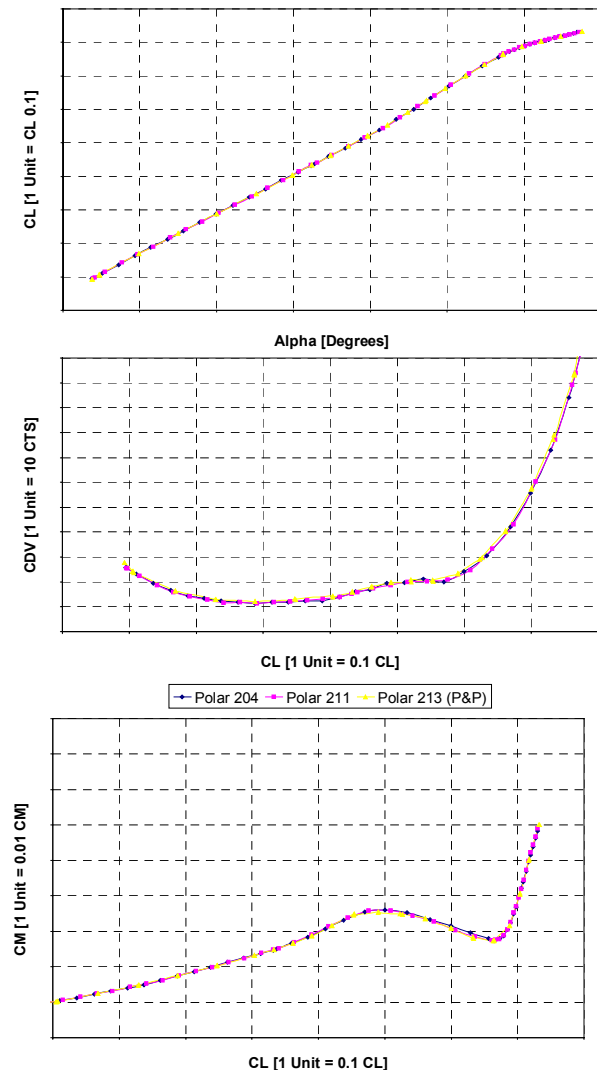


Figure 5 Short term repeatability

The levels of repeatability shown above are in line with the normal levels experienced at

ETW. In general, the repeatability in drag is around 1 drag count irrespective of the traverse type and test temperature. Equally important is the level of repeatability demonstrated by the measurement of pressures as shown in Figure 6.

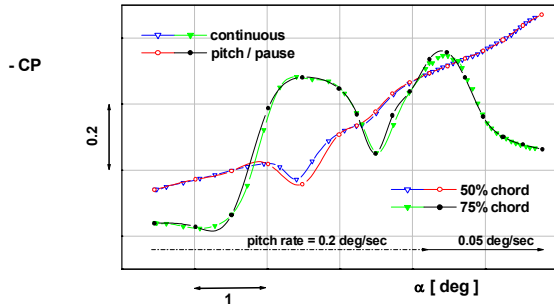


Figure 6 Short term repeatability – pressures data

Again, the levels of repeatability shown for the pressures data is consistent with general experience at ETW. From Figure 6 it can also be seen that the agreement between the pitch & pause and continuous traverses is maintained throughout the entire incidence range, primarily due to the selection of a reduced traverse rate at incidences above buffet onset.

## 2.4 Reynolds Number Effects or Aeroelastic Effects?

ETW's ability to independently control velocity, temperature, and pressure provides the capability to separate true Reynolds number effects from any pseudo Reynolds number effects. The effects of wing deformation may be investigated in detail by repeating polars at constant Reynolds number at different dynamic pressures. The test programme used for this investigation was specifically selected to separate Reynolds number effects from wing deformation effects and the following paragraphs provide a brief overview of some of the findings.

A comparison of the trailing edge pressure at two spanwise stations is provided in Figure 7. At the inboard station it can be seen that there is a noticeable variation with Reynolds number whilst there is a minimal variation with dynamic pressure. However, at the outboard station there are distinct variations with both Reynolds number and dynamic pressure.

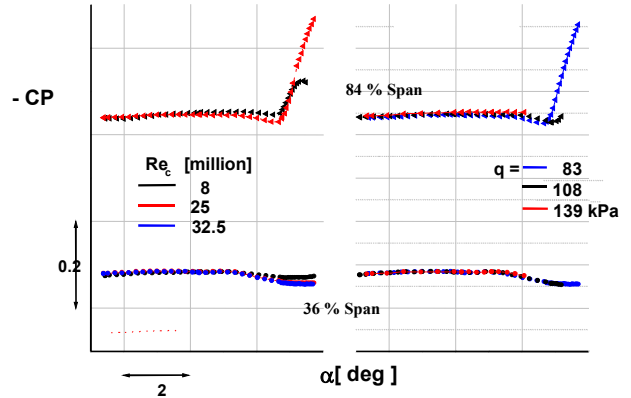


Figure 7 Trailing edge pressure characteristics

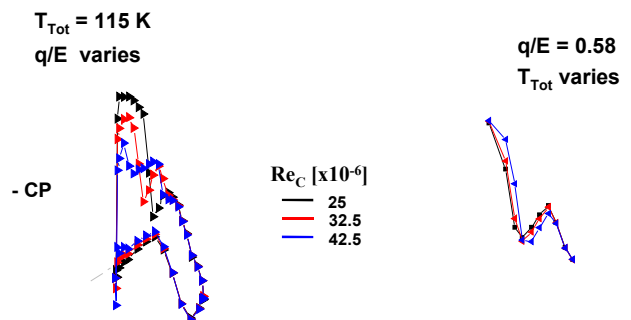


Figure 8 Pseudo and true Reynolds number effects on wing pressure distribution

Similar effects can also be seen in the complete wing pressure distributions, especially for the outboard sections, as shown in Figure 8. At the station shown there is a strong variation of the wing upper surface pressures, especially when the  $q/E$  (or wing shape) is varied to produce the change in Reynolds number. By comparison, when the same Reynolds number is achieved at nominally constant wing shape (or constant  $q/E$ ), true Reynolds number effects can be seen which are less than that given by varying tunnel  $q/E$ .

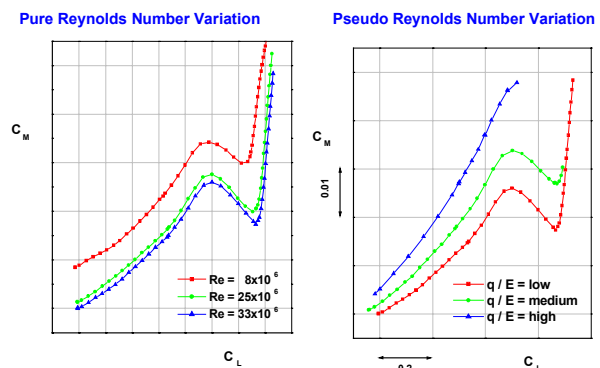


Figure 9 Pitching moment / lift characteristics

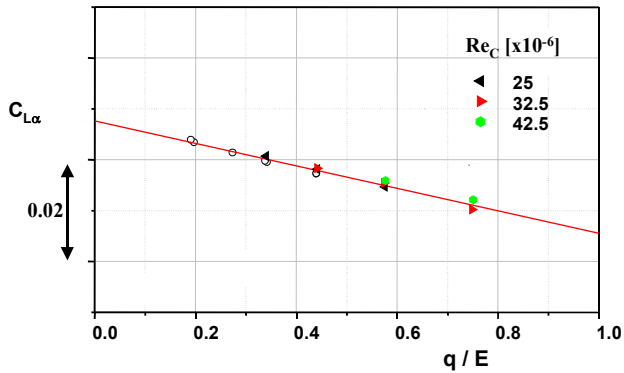


Figure 10 Aeroelastic effect on lift curve slope

Both Reynolds number and model deformation effects, as shown in Figures 9 and 10, also affect the measured forces and moments. The pitching moment characteristics show the most dramatic variations with both Reynolds number and aeroelastic effects clearly visible. The aeroelastic effects are also clearly seen in the lift curve slope characteristics whilst the associated Reynolds number effects are seen to be much smaller in comparison.

Within the complete HiReTT programme a significant amount of analysis has been undertaken to clearly separate Reynolds number effects from aeroelastic effects and the few results presented here provide the briefest of overviews. From this review it is clear that extreme caution needs to be exercised when attempting to obtain true scale effects from wind tunnel test data. Clearly, the ability to independently vary Reynolds number and dynamic pressure provides ETW's users with a distinct advantage in fully understanding scale effects. However, it is only by combining these capabilities with a well designed model and an appropriate test programme that real gains in understanding can be achieved. The issue of quantifying the actual model deformation at a particular test condition remains a difficult area and this has been addressed by supporting studies undertaken at both ETW [5] and Airbus UK [6].

### 3 Twin Sting Tests

The main objective of this part of the HiReTT programme was to establish a database

using two different measurement techniques from which sting interference effects on lift, drag, and pitching moment may be derived and subsequently applied to the single sting database described above. The first method used the 'Standard' twin sting technique to derive sting corrections from the net measurements on a split rear fuselage. The second method used the 'Enhanced' twin sting technique to derive sting corrections from the net measurements on the complete model by using newly developed twin six component balances.

### 3.1 Development of New Hardware

The twin sting tests required the development of new hardware to complement the existing model components used in the single sting tests described above. In terms of model hardware DLR Göttingen developed the following items:

- A new single piece wing incorporating twin sting attachment stub-pylons, pressure plotting, and wire routing channels.
- New live rear fuselage components incorporating a fully instrumented split plane and components to complete the fuselage representation when the dummy sting is not installed.

The new model components enabled the twin sting model representation to be geometrically similar to the single sting model whilst not introducing any significant test envelope restrictions.

In parallel with the development of the new model components NLR were tasked with the design and manufacture of two new six component balances to be installed on each of the twin sting booms together with new nose boom fairings. The balances were designed to have a combined load capacity similar to the six component performance balances used for single sting tests together with a similar accuracy requirement. The accuracy requirement of better than 0.1% full scale for each of the principal components was considered to be a significant challenge requiring comprehensive calibration over a

range of conditions. A photograph of one of the new balances attached to the TSR is provided in Figure 11.

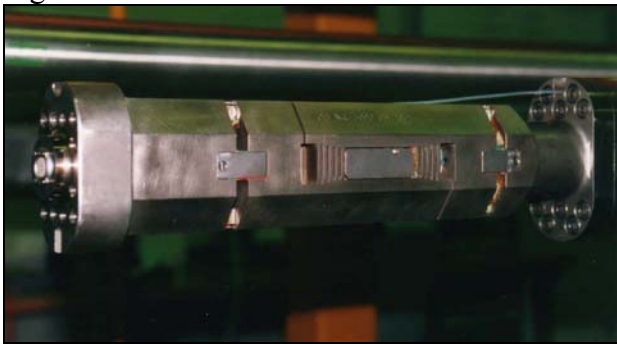


Figure 11 New boom balance installed on the TSR

The following calibration activities were undertaken for each boom balance:

- Ambient dead weight loading calibration at NLR prior to delivery to ETW
- Calibration over the complete load and temperature range using ETW’s Balance Calibration Machine [7]
- Validation check loadings at ETW using dead weights at ambient temperature

This calibration sequence is in line with normal procedures at ETW whereby it is preferable to validate calibration matrices using an independent loading method. Using this philosophy it is possible to have high levels of confidence in the calibration over the wide range of test conditions.

The fact that two individual balances are used to measure the overall model loads introduces an additional complication to the calibration activities. The behaviour of the ‘connected’ twin balances was validated by using a dummy wing which in turn was loaded using dead weights over a range of temperatures and loading conditions. The balance residuals obtained from these loading trials are shown in Figure 12 and 13 for normal force and axial force respectively. The results from these trials demonstrate that the combined output from the new boom balances closely match the applied loads over a range of test temperatures. The scatter seen in the data is primarily due to small

oscillations in the applied dead weights with axial force being particularly sensitive.

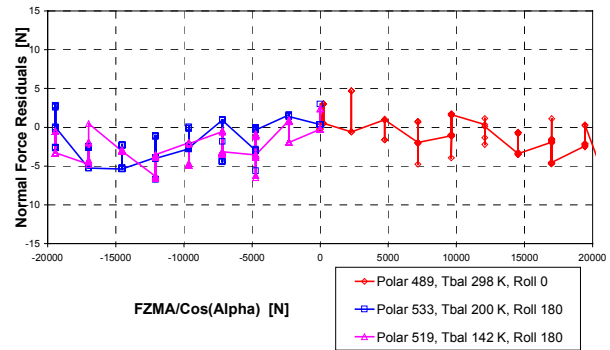


Figure 12 Combined balance normal force residuals

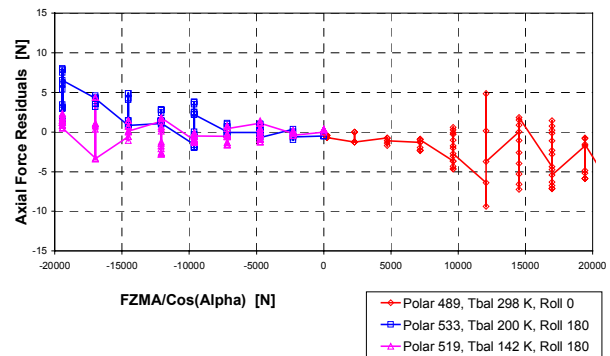


Figure 13 Combined balance axial force residuals

### 3.2 Aerodynamic Calibration

Following receipt of the new balances and their associated nose fairings it was necessary to undertake a complete aerodynamic calibration of the support system installed in ETW. A schematic of the rig together with details of the instrumentation is provided in Figure 14.

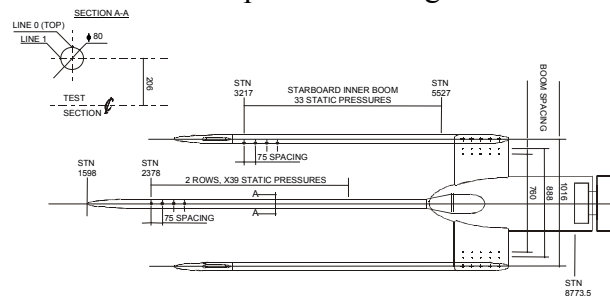


Figure 14 Aerodynamic calibration set-up

From Figure 14 it can be seen that the primary calibration device is a centrally supported axial probe incorporating two rows of pressure tappings. These tappings are subsequently used to derive the pressure

gradient along the centre line of the support system in the vicinity of the model volume. Typical test conditions selected for the calibration of the TSR support system are shown in Figure 15.

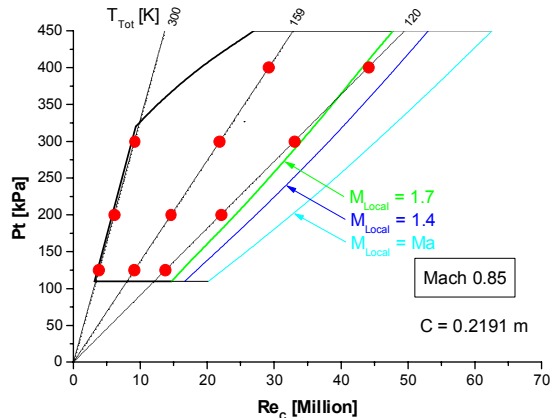


Figure 15 Calibration envelope for the twin sting rig

From Figure 15 it can be seen that for Mach 0.85 the calibration matrix includes three temperature levels and four pressure levels. Similar parameter ranges are also covered throughout the entire subsonic speed range. This calibration matrix typifies the extent to which ETW normally calibrates the various test section configurations. A sample of the raw data produced at all test conditions is provided in Figure 16. From this figure it can be seen that the calibration is largely independent of temperature and pressure variations and is therefore insensitive to Reynolds number variations. This result is similar to previous calibration campaigns with the ‘empty test section’ where the slotted walls of the test section produce calibration characteristics insensitive to Reynolds number.

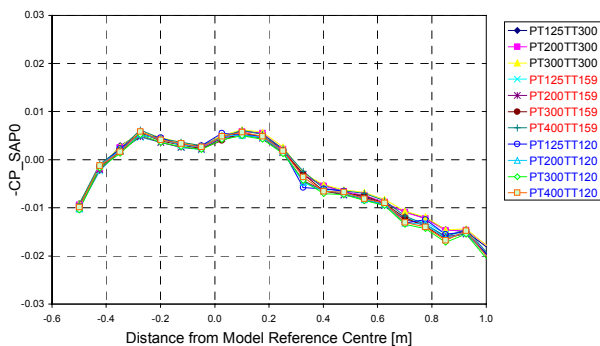


Figure 16 Pressure distribution along calibration probe

Figure 17 provides the derived pressure characteristics for the TSR ‘in isolation’ following all post-processing activities. The post processing included corrections to Mach number at the model moment reference centre together with a correction for the direct effect of the short axial probe based on potential flow considerations.

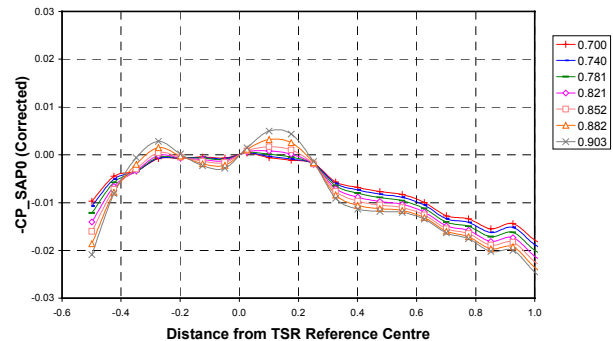


Figure 17 Corrected pressure distribution

### 3.3 Sting Correction Test Overview

The twin sting tests were split into two phases covering the different test techniques to be examined as part of the HiReTT programme:

- The first phase used the ‘standard’ twin sting test technique where the sting corrections are derived by measuring the net forces on a live rear fuselage with and without a dummy sting.
- The second phase used the ‘enhanced’ twin sting test technique where the sting corrections are derived from the overall forces and moments measured on the complete model by the twin boom balances with and without a dummy sting.

During each phase the model was tested at many of the conditions covered by the single sting test series defined in Figure 2; the only notable exceptions were the omission of the intermediate transition fixed conditions and the  $q/E=0.75$  transition free conditions.

A general view of the model installed on the twin sting rig during the pre-test preparations is provided in Figure 18. An impression of the relative sizes of the model / twin sting rig / dummy sting can be gained from this photograph.



Figure 18 Model installed on the twin sting rig

### 3.4 Split Fuselage Characteristics Obtained from the Standard TSR Technique

The instrumentation used to measure the net forces comprised an internal balance together with a pressure measurement system used to determine the forces acting at the split plane and, in the case of the dummy sting on configurations, the base cavity region. The net forces also include a contribution from the rig buoyancy derived from the aerodynamic calibration activities described above.

An example breakdown of the relevant contributions to the overall drag characteristics is provided in Figure 19. From this figure it can be seen from the relative magnitudes that all measurements need to be made to the highest accuracy standards to enable reliable sting correction increments to be obtained.

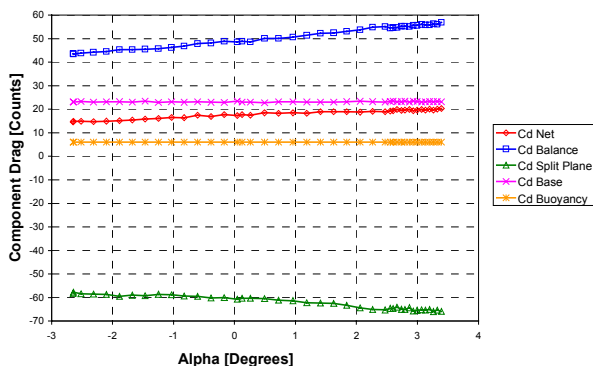


Figure 19 Rear fuselage drag contributions

A number of repeat conditions were built into the test programme to confirm data quality.

Figure 20 provides a comparison of three polars acquired at Mach 0.85 at  $Rc=32.5$  million, polars 260 and 265 used the continuous traverse technique and polar 267 used the pitch & pause technique.

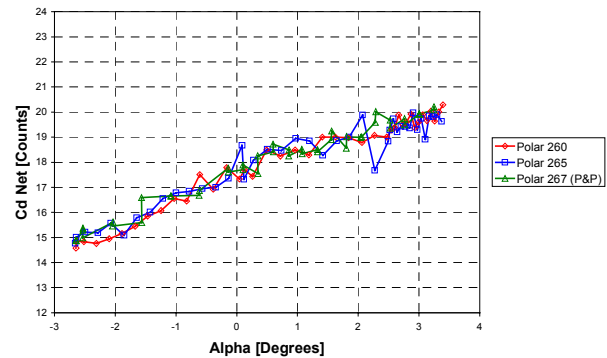


Figure 20 Short-term drag repeatability

### 3.5 Solid Fuselage Characteristics Obtained from the ‘Enhanced’ TSR Technique

Prior to the start of this phase of the programme the split rear fuselage was converted to a ‘solid fuselage’ by replacing the internal balance with a dummy balance and by inserting a filler component to complete the external geometry. This subtle modification was necessary to eliminate any cross flow or recirculation effects that may be introduced when a split plane is inserted.

The instrumentation used to measure the overall forces and moments comprised the two new boom balances together with pressure measurement systems used to determine the forces acting on the boom balance cavities and, in the case of the dummy sting on configurations, the base cavity region. The overall forces also included a contribution from the rig buoyancy derived from the aerodynamic calibration activities described above. For this “live complete model” method, provision was made to maintain the model weight distribution (and hence the wing twist shape) between the dummy sting on and off tests.

An example of the drag increment repeatability is provided in Figure 21 and 22 for both low and high Reynolds number conditions. These drag increments represent the difference between a configuration with a distorted afterbody / sting cavity / dummy sting



representation and a configuration with a full afterbody representation without a dummy sting. The repeatability is demonstrated by differencing all combinations of repeat continuous polars at the selected test conditions. From these figures it can be seen that the general level of uncertainty demonstrated by the ‘Enhanced’ TSR technique is better than 1 drag count irrespective of Reynolds number, and therefore a similar order of magnitude to that demonstrated in the earlier single sting test series.

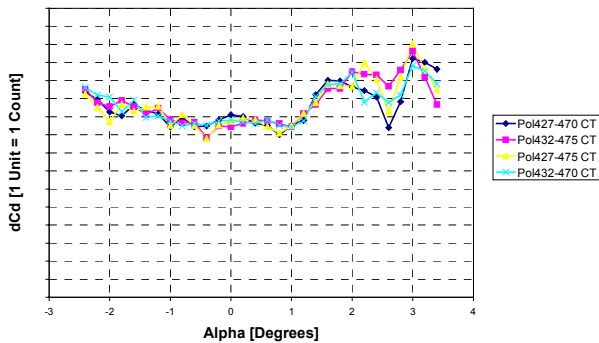


Figure 21 Repeatability at low Reynolds number

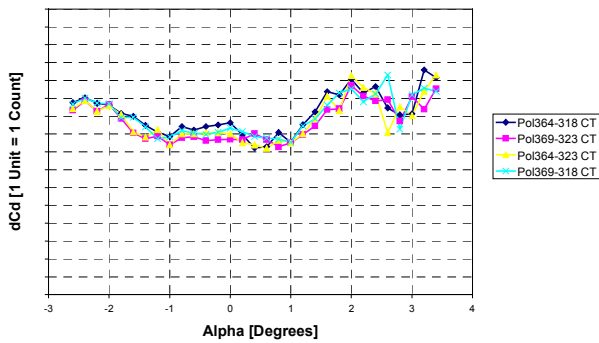


Figure 22 Repeatability at high Reynolds number

The low levels of uncertainty demonstrated within the sting interference part of the HiReTT programme are considered to be an excellent starting point for the new ‘Enhanced’ TSR technique.

### 3.6 TSR Technique Comparison

Both the ‘Standard’ and ‘Enhanced’ TSR techniques have demonstrated similar levels of repeatability and the resultant sting interference increments have similar levels of overall data uncertainty. When considered in isolation each

technique produced a consistent set of sting interference increments over the complete range of test conditions. However, a direct comparison of the two techniques showed differences that may be attributable to the close-coupled nature of the configuration being used for the HiReTT programme. Differences between the techniques were not completely unexpected and ongoing investigations should lead to a better understanding of the relative merits of these techniques.

## 4 Conclusions

Two test series have been successfully completed at ETW as part of the comprehensive HiReTT research programme to investigate a modern transport aircraft configuration over a large range of Reynolds numbers. The first test series provided a high quality single sting dataset covering a range of Reynolds numbers from 4-42 million suitable for separating Reynolds number effects from aeroelastic effects. The second test series provided complementary sting interference datasets derived from both the existing standard twin sting technique and the newly developed enhanced twin sting technique. The techniques described in this paper provide ETW’s users with the ability to derive high speed, high quality, high Reynolds number performance data with inherent low levels of data uncertainty.

## Acknowledgements

The authors wish to thank the many organizations that have made positive contributions to the parts of the HiReTT programme described in this paper. The HiReTT programme is part funded through the European Commission 5<sup>th</sup> Framework programme. Thanks are also due to staff at ETW who have contributed significantly to the successful calibration, integration, and development of the enhanced twin sting technique.

## References

- [1] Rolston S. *Initial Achievements of the European High Reynolds Number Research Project 'HiReTT'*. AIAA-2002-0421
- [2] Rolston S. *High Reynolds Number Tools and Techniques for Civil Aircraft Design – an Overview of the HiReTT Programme*. Air & Space Europe, Volume 3, 2001
- [3] White PJ, Price IAC, Sale RS, Simmons MJ. *Overcoming the Challenges of Designing, Manufacturing, and Testing of Cryogenic Wind Tunnel Models*. ICAS-2000-372, Harrogate
- [4] Ansell DM, Schimanski D. *Non-Intrusive Optical Measuring Techniques Operated in Cryogenic Test Conditions at the European Transonic Windtunnel*. AIAA-1999-0946
- [5] Gross N. *ETW Analytical Approach to Assess the Wing Twist of Pressure Plotted Wind Tunnel Models*. AIAA-2002-0310
- [6] Gibson T. *Investigation of Wind Tunnel Model Deformation under High Reynolds Number Aerodynamic Loading*. AIAA-2002-0424
- [7] Jansen U. *Automatic Cryogenic Balance Calibrations at ETW - Pushing the Limits*. 3<sup>rd</sup> International Symposium on Strain Gauge Balances, Darmstadt, May 2002